J. Plasma Physics (2011), *vol.* 77, *part* 2, *pp.* 257–263. © Cambridge University Press 2010
doi:10.1017/S0022377810000206

Stability of an electron beam in a two-frequency wiggler with a self-generated field

SOON-KWON NAM[1] and KI-BUM KIM[2]

[1]Department of Physics, Kangwon National University, Chunchon 200-701, Republic of Korea
(snam@kangwon.ac.kr)

[2]Cyclotron Research Institute, Kangwon National University, Chunchon 200-701, Republic of Korea
(kkbum@kangwon.ac.kr)

(Received 6 January 2010 and accepted 24 March 2010, first published online 27 April 2010)

Abstract. We investigate the relativistic electron motions in a two-frequency wiggler magnetic field with self-generated fields. The equations of motion are derived from the Hamiltonian which include the self-generated field, and we find the steady-state orbit from the equations of motion. The stability of electron motion in a two-frequency wiggler is examined by the numerical simulation. We analyze the a dynamical systems using the fast Fourier transformation and the Poincarè surface of section to find the critical value which have the periodical electron motion and to optimize the two-frequency wiggler.

1. Introduction

The free-electron laser is the powerful electromagnetic generation source, and has many remarkable advantages such as frequency tunability from microwave to X-ray, high power, and high efficiency [1, 2]. To get the high power radiation for the basic research and applications, the free-electron laser is operated in the high electron beam current and high-magnetic field. In the high-gain region, the stability of electron beam plays an important role and limits the operating wavelength, gain, and efficiency in a free-electron laser operation [3–6].

The intensity of the radiation are reduced because of the betatron oscillation and instability of electron beam. Therefore, the stability of electron beam is important to get the high efficiency and the gain in the high-power free-electron laser. To preserve the stability of electron beam and to enhance the efficiency and the gain, the two-frequency wiggler [7–9] was used.

The high-power far-infrared radiation which have wavelength between 30 μm and 1 mm has many applications in the field of spectroscopy, solid-state physics, biology, and medicine. We plan to construct free-electron laser facility beside Cyclotron facility in Kangwon National University (KNU), and it will operate in the far-infrared region.

In this work, we study the stability of electron motion in the two-frequency wiggler magnetic field and self-generate fields which are induced from propagated electron

https://doi.org/10.1017/S0022377810000206 Published online by Cambridge University Press

beam with high current in the high-power far-infrared free-electron laser. We analyze the electron motion due to the high wiggler magnetic field and self-generate fields by the numerical simulation. The betatron oscillation and stability of electron beam are studied using spectrum analysis and Poincarè surface of section, and we find the optimized condition of two-frequency wiggler.

2. Theoretical model

When the free-electron laser operates in the high-current region to get the high gain, the space charge and the current of the electron beam generate self-electric and self-magnetic fields [11–14]. In the steady state, Maxwell's equations are $\nabla \cdot \mathbf{E} = 4\pi\rho_0$ and $\nabla \times \mathbf{B} = 4\pi\mathbf{J}/\mathrm{c}$, and it can define the self-generated electric field and the self-generated magnetic field which induced from the charge density and the current density of the electron beam.

We assume that the equilibrium properties, which are the density n_b and mean velocity $\bar{v}_b$ of electron are uniform in the z direction with $\partial n_b/\partial z = 0$ and $\partial \bar{v}_b/\partial z = 0$. The radial density and the velocity profiles are assumed to be azimuthally symmetric about the z-axis. Therefore, the density and the velocity profiles can be written as only functions of r, and Maxwell's equations in cylinderical coordinate system become

$$\nabla \cdot \mathbf{E_s}(\mathbf{r}) = \frac{1}{r}\frac{\partial}{\partial r}\big(rE_s(r)\big) = 4\pi\rho_0(r), \tag{2.1}$$

$$\nabla \times \mathbf{B_s}(\mathbf{r}) = \frac{1}{r}\frac{\partial}{\partial r}\big(B_s(r)\big)\hat{e}_z = \frac{4\pi}{c}J_z(r)\hat{e}_z, \tag{2.2}$$

where $\rho_0(r) = -ef_b(r)$ is charge density, $J_z(r) = -f_b(r)e\bar{v}_z$ is axial current density, and $f_b(r)$ is electron beam profile function.

The electron beam is assumed to have a uniform density profile, such as

$$f_b(r) = \begin{cases} n_b, & 0 \leqslant r < r_b, \\ 0, & r > r_b, \end{cases} \tag{2.3}$$

where n_b is the electron density and r_b is the electron beam radius. The self-generated electric field $E_s(r)$ induced by the space charge, and azimuthal self-magnetic field $B_s(r)$ induced by the axial current are founded by the steady-state Maxwell equations

$$E_s(r) = -\frac{4\pi e}{r}\int_0^r r' f_b(r')dr'\hat{e}_r = -2\pi e n_b r\hat{e}_r, \tag{2.4}$$

$$B_s(r) = -\frac{4\pi e}{r}\int_0^r r' f_b(r')\beta_z(r')dr'\hat{e}_\theta = -2\pi e n_b r\beta_z\hat{e}_\theta, \tag{2.5}$$

where $\beta_z = \bar{v}_z/c$, $\bar{v}_z$ is the average axial velocity of the electron beam, and c is the velocity of light.

The scalar potential and vector potential of the self-generated field in Cartesian coordinate system, which satisfies $\mathbf{E_s} = -\nabla\Phi_s$ and $\mathbf{B_s} = \nabla \times \mathbf{A_s}$, are

$$\Phi_s = \frac{m_e\omega_p^2}{4e}(x^2 + y^2), \tag{2.6}$$

$$\mathbf{A_s} = \Phi_s\beta_z\hat{e}_z, \tag{2.7}$$

https://doi.org/10.1017/S0022377810000206 Published online by Cambridge University Press

where $\omega_p = \sqrt{4\pi n_b e^2/m_e^2}$ is the plasma frequency of the electron beam, m_e is the electron rest mass, and e is the electron charge.

The two-frequency wiggler magnetic field is defined as [10]

$$\mathbf{B_w} = (1-\rho)B_{w0}\cosh(k_w x)\cos(k_w z) + \rho B_{w0}\cosh(k_w z)\cos(3k_w z), \tag{2.8}$$

where $\lambda_w = 2\pi/k_w$ is the wiggler period, B_{w0} is a magnetic field strength of wiggler in the electron beam center, and ρ is the two-frequency ratio parameter.

The Hamiltonian of relativistic electron is

$$\mathbf{H} = \sqrt{(c\mathbf{P} + e\mathbf{A})^2 + m_e^2 c^4} - e\Phi_s \equiv \gamma m_e c^2 - e\Phi_s, \tag{2.9}$$

where $\gamma = \sqrt{1 + (\mathbf{p}/m_e c)^2}$ is the relativistic mass factor.

The total vector potential is $\mathbf{A} = \mathbf{A_w} + \mathbf{A_s}$, $\mathbf{A_w}$ is the vector potential of two-frequency wiggler which is satisfied $\mathbf{B_w} = \nabla \times \mathbf{A_w}$, $\mathbf{P}$ is the canonical momentum, and $\mathbf{p} = \mathbf{P} + e\mathbf{A}/c$ is the mechanical momentum. For notation convenience, we introduce the dimensionless scalar potential $\bar{\Phi}_s = e\Phi_s/m_e c^2 k_w$, the dimensionless vector potential $\bar{\mathbf{A}} = e\mathbf{A}/m_e c^2 k_w$, the dimensionless canonical momentum $\bar{\mathbf{P}} = \mathbf{P}/m_e c$, and the dimensionless wiggler magnetic field amplitude $a_{w0} = eB_{w0}/m_e c^2 k_w$. The dimensionless Hamiltonian defined by

$$\bar{\mathbf{H}} = \frac{\mathbf{H}}{m_e c^2} = \sqrt{(\bar{\mathbf{P}} + \bar{\mathbf{A}})^2 + 1} - \bar{\Phi}_s = \gamma - \bar{\Phi}_s. \tag{2.10}$$

3. Analysis of stability of the electron motions

We assume that the y component of canonical momentum are exact constant of the motion, therefore, we interest the (x, z) plan only. The equation of motion for a relativistic electron can be derived from the Hamiltonian. Since Hamiltonian is independent of time, the electron motions can be described in the $(k_w z, \bar{P}_x, \bar{P}_z)$ phase space [15].

The stability of electron beam in the two-frequency wiggler are studied by using a spectral analysis of electron trajectory, and Poincarè surface of section plot. In this studies, we use the 8 m long wiggler with the wiggler period $\lambda_w = 4$ cm and wiggler parameter $a_{w0} = 6$ which corresponds to wiggler magnetic field strength $B_{w0} = 16$ Kg. The energy of incident electron beam E_b is 15 MeV ($\gamma = 39.1$), and the electron beam current I_b is 210 A.

Figure 1 shows the electron trajectories of x-axis and fast Fourier transformation for various initial transverse position of electron $k_w x_0$ in conventional wiggler with $\rho = 0$. The electron orbit has a regular motion for $k_w x_0 = 1.3$, but the electron orbit become unstable as the initial transverse position increases, as shown in Fig. 1(c,d).

To study the periodicity of the electron motion, the fast Fourier transformation are calculated for various $k_w x_0$ as shown in Fig. 2. For conventional wiggler, the periodicity of the electron motion disappears when the initial transverse position exceeds $k_w x_0 = 1.8$, but its value increases to $k_w x_0 = 2.0$ in the two-frequency wiggler with $\rho = 0.6$.

Figure 3 shows the Poincarè surface of section plot in the $(k_w z, \bar{P}_z)$ plane at $\bar{P}_x = 0$ for the conventional wiggler and two-frequency wiggler with $\rho = 0.6$. As $k_w x_0$ increases, the contour size of Poincarè surface of section increases, and the

https://doi.org/10.1017/S0022377810000206 Published online by Cambridge University Press

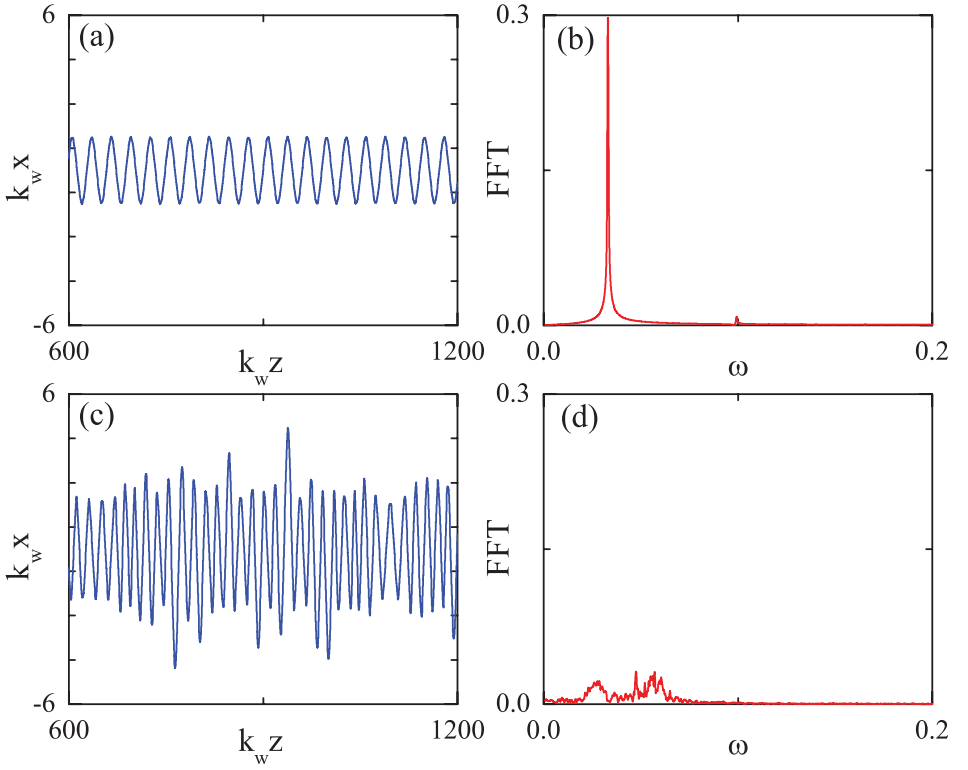


Figure 1. (Colour online) The transverse motions of electron and its fast Fourier transformation for (a, b) the stable region at $k_w x_0 = 1.3$ and (c, d) the unstable region at $k_w x_0 = 1.9$. Other parameters are $B_{w0} = 16\ kG$, $I_b = 210\ A$, and $\rho = 0$.

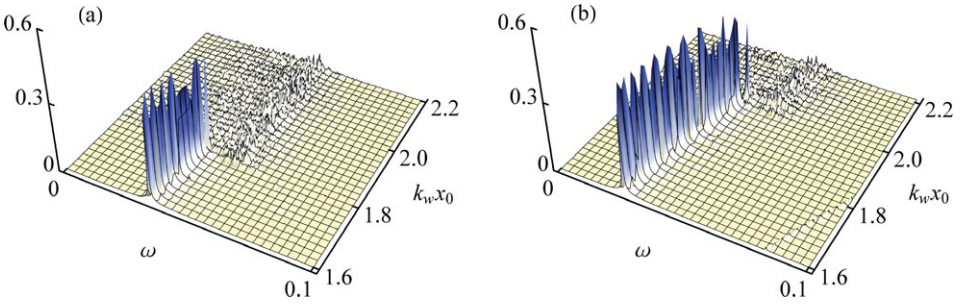


Figure 2. (Colour online) The fast Fourier transformation of electron transverse motion versus initial transverse position($k_w x_0$) for (a) $\rho = 0$ and (b) $\rho = 0.3$.

contour disappears when $k_w x_0$ exceeds critical value. It means that the amplitude of betatron oscillation increases, and the coupling between sinusoidal electron motion and betatron oscillation becomes stronger. Figure 4 shows Poincarè surface of section plots for various two-frequency wiggler ratio parameter ρ. Those critical values of $k_w x_0$ which have the periodical electron motion are correspond to the results of Fig. 2.

https://doi.org/10.1017/S0022377810000206 Published online by Cambridge University Press

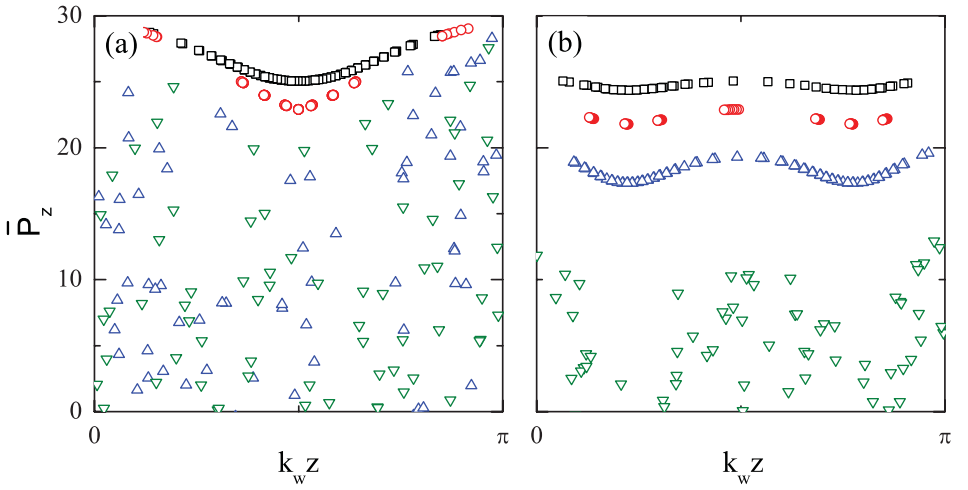


Figure 3. (Colour online) Poincarè surface of section plot in the $(k_w z, \bar{P}_z)$ plane at $\bar{P}_x = 0$ for (a) $\rho = 0$ and (b) $\rho = 0.6$: (□) $k_w x_0 = 1.6$, (○) $k_w x_0 = 1.8$, (△) $k_w x_0 = 2.0$, and (▽) $k_w x_0 = 2.2$.

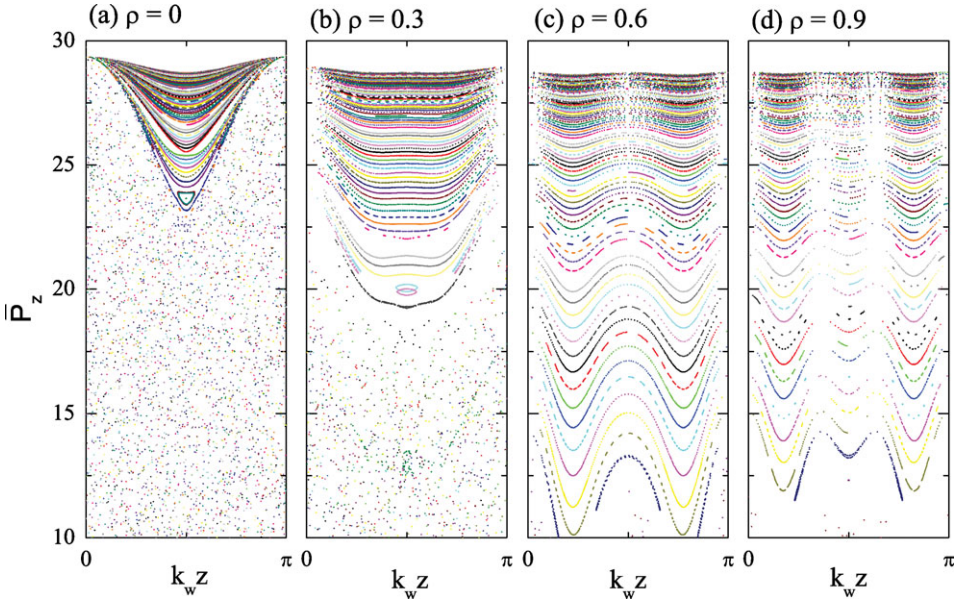


Figure 4. (Colour online) Poincarè surface of section plots in the $(k_w z, \bar{P}_z)$ plane at $\bar{P}_x = 0$ for various initial transverse displacement: (a) $\rho = 0$, (b) $\rho = 0.3$, (c) $\rho = 0.6$, and (d) $\rho = 0.9$.

The stability of electron motion for various ρ and $k_w x_0$ is shown in Fig. 5. The stable region of electron motion is broadened with increasing ρ, and it is optimized at $\rho = 0.6$. Using optimized two-frequency wiggler, the stable region of $k_w x_0$ increases about 15% compared with that of the conventional wiggler.

https://doi.org/10.1017/S0022377810000206 Published online by Cambridge University Press

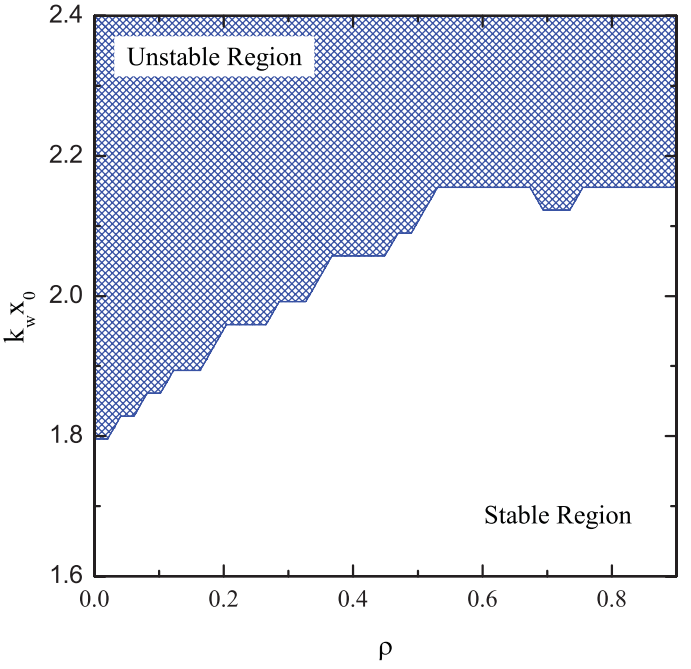


Figure 5. (Colour online) The region of stable motion in the electron orbit for various the initial transverse displacement $k_w x_0$ and the two-frequency wiggler ratio parameter ρ.

4. Conclusions

To enhance the efficiency and the gain in the high-power far-infrared free-electron laser, we investigated the electron beam dynamics in the two-frequency wiggler magnetic field with self-generated electric and magnetic fields. The equations of motion were derived by using a Hamiltonian included self-generated field. The periodicity and stability of the electron motion were studied using spectrum analysis and Poincarè surface of section, and we found the optimized condition of the two-frequency wiggler to preserve the stability of electron beam. When the two-frequency wiggler was optimized, the stable region of $k_w x_0$ was increased about 15% compared with that of the conventional wiggler. This method is expected to enhance the efficiency and the gain in a high-power free-electron laser.

Acknowledgements

This work was supported by the Cyclotron Research Institute at Kangwon National University, Chuncheon, Korea.

References

[1] Benson, S. V. and Madey, J. M. J. 1989 Demonstration of harmonic lasing in a free-electron laser. *Phys. Rev.* A **39**, 1579–1581.

[2] Luchini, P. and Motz, H. 1990 *Undulators and Free-electron Lasers*. New York: Oxford University Press.

https://doi.org/10.1017/S0022377810000206 Published online by Cambridge University Press

[3] Mishra, G., Basu, C., Chouhan, S., Dutta, A. K. and Rajput, N. P. 2003 Betatron harmonic radiation from crossed-planar undulators used in low-energy FELs. *J. Mod. Opt*. **50**(8), 1299–1308.

[4] Chouhan, S. and Mishra, G. 2002 Effects of inhomogeneous broadening on two-frequency longitudinal wiggler brightness. *Phys. Lett*. A **299**(4), 392–400.

[5] Dattoli, G. and Bucci, L. 2002 Free electron lasers operating with variably polarization undulators. *Nucl. Instrum. Methods Phys. Res*. A **450**, 479–490.

[6] Nam, S.-K. and Kim, K.-B. 2005 The stability of an electron beam in a free-electron laser with a tapered helical wiggler. *J. Korean Phys. Soc*. **47**, 958–963.

[7] Yang, Y. and Ding, W. 1998 Enhanced harmonic radiation from a dual-harmonic wiggler. *Nucl. Instrum. Methods Phys. Res*. A **407**, 60–63.

[8] Dattoli, G., Giannessi, L., Ottaviani, P. L., Freund, H. P., Biedron, S. G. and Milton, S. 2002 Two harmonic undulators and harmonic generation in high gain free electron lasers. *Nucl. Instrum. Methods Phys. Res*. A **495**, 48–57.

[9] Gupta, V. and Mishra, G. 2006 Harmonic undulator free electron laser and betatron oscillations . *Nucl. Instrum. Methods Phys. Res*. A **556**, 350–356.

[10] Iracane, D., Touati, D. and Chaix, P. 1994 Effect of the wiggler harmonics on the free electron laser dynamics. *Nucl. Instrum. Methods Phys. Res*. A **341**, 220–224.

[11] Michel, L., Bourdier, A. and Buzzi, J. M. 1991 Chaotic electron trajectories in a free electron laser . *Nucl. Instrum. Methods Phys. Res*. A **304**, 465–471.

[12] Spindler, S. and Renz, G. 1991 Chaotic behavior of electron orbits in a free electron laser near magnetoresonance. *Nucl. Instrum. Methods Phys. Res*. A **304**, 492–496.

[13] Michel-Lours, L., Bourdier, A. and Buzzi, J. M. 1993 Chaotic electron trajectories in a free-electron laser with a linearly polarized wiggler. *Phys. Fluids* B **5**, 965–971.

[14] Bourdier, A. and Michel-Lours, L., 1994 Identifying chaotic electron trajectories in a helical-wiggler free-electron laser. *Phys. Rev*. E **49**, 3353–3359.

[15] Chen, C. and Davidson, R. C. 1990 Chaotic electron dynamics for relativistic-electron-beam propagation through a planar wiggler magnetic field. *Phys. Rev*. A **42**, 5041–5044.

https://doi.org/10.1017/S0022377810000206 Published online by Cambridge University Press